Detecting galaxy clusters and measuring their mass with weak gravitational lensing.

Joel Bergé (1) and Alexandre Réfrégier (2)
(1) Jet Propulsion Laboratory / Caltech / CEA Saclay
(2) CEA Saclay

Abstract : We show how weak gravitational lensing will allow us to detect and weigh clusters of galaxies. We compare the merits of ground-based and space-based surveys, by showing the selection function they provide. We show the number of clusters that can be detected with weak lensing, and the accuracy that we can reach while measuring their individual mass. We then show how to stack X-ray clusters, even if they are not detectable through their weak lensing signal, in order to improve the accuracy in their average gravitational mass measurement.

Weak gravitational lensing, through the coherent distorsion it produces on background galaxies, due to mass overdensities, allows one to efficiently detect and map dark matter. For instance, one can use it to map the distribution of clusters of galaxies. Moreover, as weak lensing only depends on the matter distribution, and not on its physical state, it is well suited to measure galaxy clusters' mass without prior on their subjacent physics.

We show how a survey strategy affects the capability of weak lensing to detect and weigh galaxy clusters. In Figure 1, we show the main effect of the seeing : the number density of background galaxies will vary with seeing. The seeing also affects the shape measurement error for galaxies, but for simplicity we decided not to take this effect into account. The weak lensing selection function depends on the number density of background galaxies n_g and on the median redshift z_m of their distribution, and is shown on Fig. 2 for three different surveys. Figure 3 shows the redshift distribution of clusters of galaxies that can be detected through their weak lensing signal, depending on the survey's characteristics and detection threshold.

We show how we are able to measure the mass of a cluster of galaxies with its weak lensing signal, in Fig. 4. The relative error made on a cluster's mass measurement is the inverse of its signal-to-noise ratio. Most galaxy clusters cannot be weighted individually with an accuracy better than 20% to 50%, depending on the survey's specification (n_g and z_m). Figure 5 shows the number of clusters that can be detected, using different surveys, in the redshift-mass plane. In particular, that figure shows where the whole population of clusters lies in this plane. Weak lensing clearly does not detect all of them. Assuming that they are all (down to a given mass) detectable with their X-ray signal, it becomes possible to stack their weak lensing signals so as to be able to measure an average mass for halos lying in the same region of the redshift-mass plane. Doing so, we can lower the error on the mass measurement by $\sqrt{N}$, where N is the number of clusters that we stack. Figure 6 shows the accuracy on the average mass that we are able to reach, depending on the survey's characteristics. Using current ground-based surveys, we can reach 15% accuracy on the average mass of halos ranging between $10^{13}h^{-1}M_\odot$ and $2\times10^{14}h^{-1}M_\odot$, and with redshift comprised between $z=0.2$ and $z=0.6$, if using a 50 deg^2 CFHTLS Wide-like survey. Increasing its area to 200 deg^2 allows us to reach 7% accuracy on the

mass measurement of the same clusters. Same surface surveys, but based on Subaru specifications, will allow us to reach 7% and 4% accuracy, respectively. A space-based, SNAP-like survey, of area 1000 deg^2, will lower the accuracy to 1%, and a DUNE-like survey, with an area increased up to 20000 deg^2, will allow us to reach a 0.3% accuracy on the average mass of galaxy clusters.

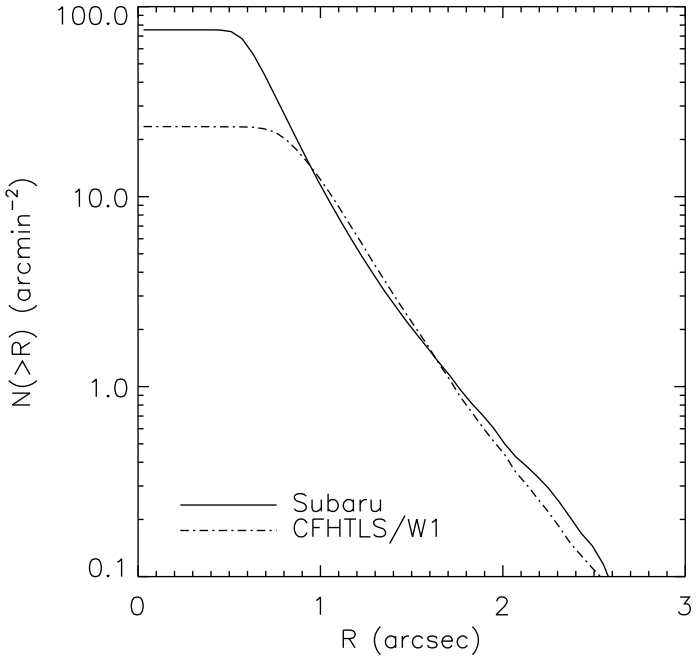

Figure 1: Effect of the seeing on the number density of useful galaxies in a weak lensing analysis. The lines show the cumulative distribution of galaxies size in a typical Subaru image (solid line, [2]) and in a typical CFHTLS Wide image (dash-dot, [1]). The size R shown here is defined as the FWHM of galaxies, for a direct comparison with the PSF FWHM, which defines the seeing. The distribution flattens for R $<$ seeing, since galaxies smaller than the PSF are not useable. The smaller the PSF (FWHM$_{\rm Subaru} \approx 0.5$ arcsec, FWHM$_{\rm CFHTLS} \approx 0.7$ arcsec), the higher the number density of small galaxies, and the higher the number density of useable galaxies. Note that the size distribution of big galaxies scale roughly the same in Subaru and CFHTLS Wide data. Beside the galaxies selection effect showed by this figure, the seeing affects the achievable accuracy on shape measurement, and thus affects the rms error in shear measurement σ_γ. For simplicity, we will ignore this effect in the following, and will assume $\sigma_\gamma = 0.3$ for all surveys.

Table 1: Surveys considered hereafter. The first two are drawn from the CFHTLS Wide survey (e.g. [1]), assuming different sky coverage. We assume Subaru characteristics, with different areas, for surveys 3 and 4. Surveys 5 and 6 are drawn from SNAP and DUNE, respectively. Surveys 1 through 4 are ground-based surveys, whereas the last two are space-based surveys. The definition of those surveys allows us to explore the effect of n_g, z_m and the survey's area on weak lensing measurements.

Survey ID	Type	n_g (arcmin^{-2})	z_m	Area (deg^2)
1	CFHTLS Wide	10	0.8	50
2	CFHTLS Wide	10	0.8	200
3	Subaru	30	0.9	50
4	Subaru	30	0.9	200
5	SNAP	70	1.2	1000
6	DUNE	40	1.1	20000

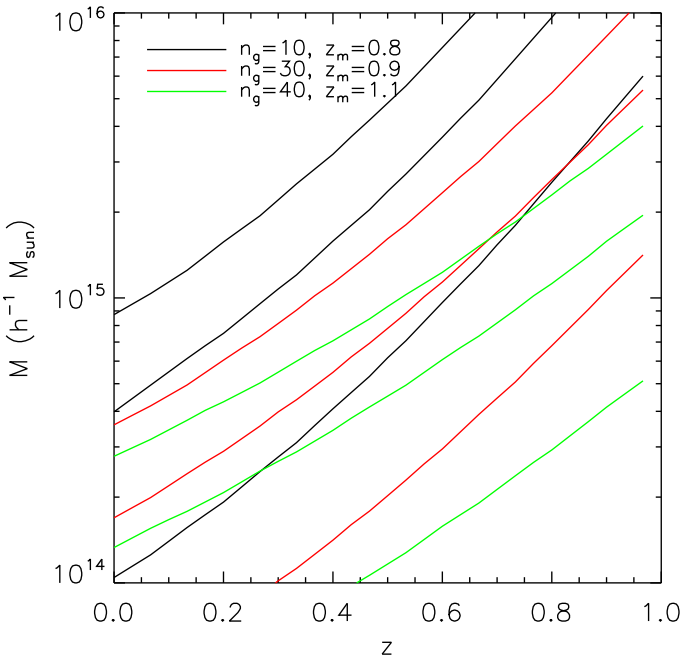

Figure 2: Weak lensing selection function (at 3σ, 7σ and 11σ from bottom to top for each color), in the redshift-mass plane, as defined in [1]. Each color codes for a different survey, characterized by its galaxy number density n_g and its median redshift z_m (black : surveys 1-2 ; red : surveys 3-4 ; green : survey 6 of Table 1), the selection function being independent of the survey's area. Increasing the galaxy number density lowers the lowest detectable mass. Increasing the median redshift flattens the slope of the selection function, since farther galaxies become useable. The redshift distribution of background galaxies is parametrized by a three-parameter parametrization [5], in which we only vary z_m here.

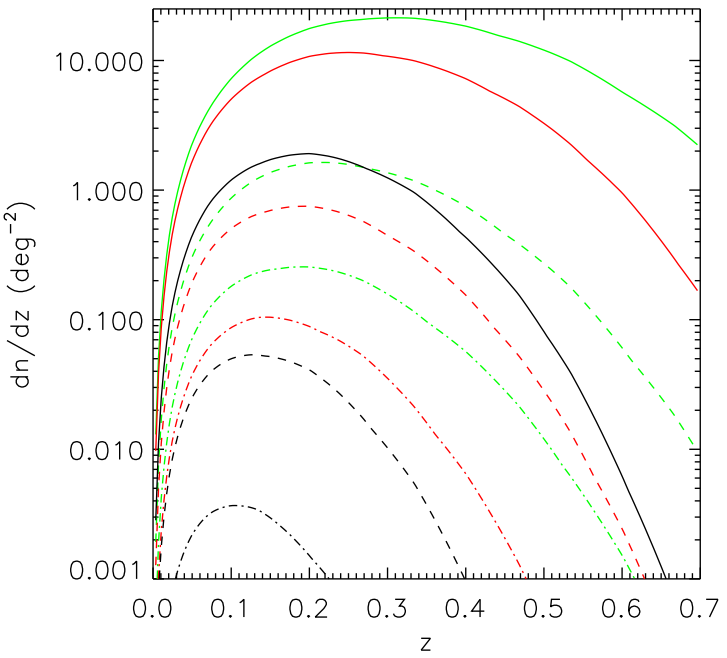

Figure 3: Distribution of detectable galaxy clusters, per unit of redshift and solid angle, for the same surveys characteristics as that of Fig. 2, with the same color code. Solid lines show the number of clusters that one can detect through their weak lensing signal, at the 3σ detection level. Dashed lines show the same quantity, at the 7σ level, and dash-dot lines at the 11σ level. At a given detection threshold, the bigger n_g, the more numerous the detected halos ; the bigger z_m, the bigger the detected halos' mean redshift. We used a Jenkins mass function to compute $\mathrm{d}n/\mathrm{d}z$ [3].

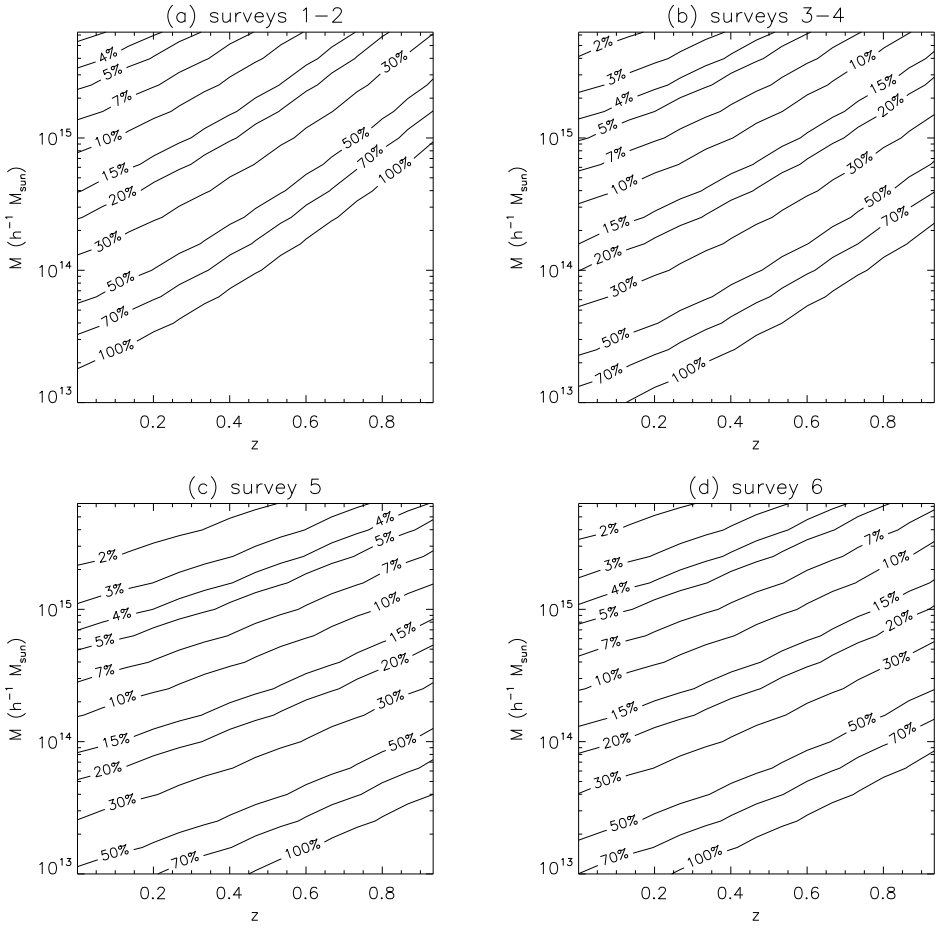

Figure 4: Relative error that can be reached on a single cluster's mass measurement from its weak lensing effect, in the redshift-mass plane. This error simply scales as $1/\nu$, where ν is the signal-to-noise ratio created by a single halo, defined as M/σ_M, where M is the mass of the halo and σ_M the error made on its measurement. Contours are shown for the surveys defined in Table 1 : (a) surveys 1-2 ; (b) surveys 3-4 ; (c) survey 5 ; (d) survey 6.

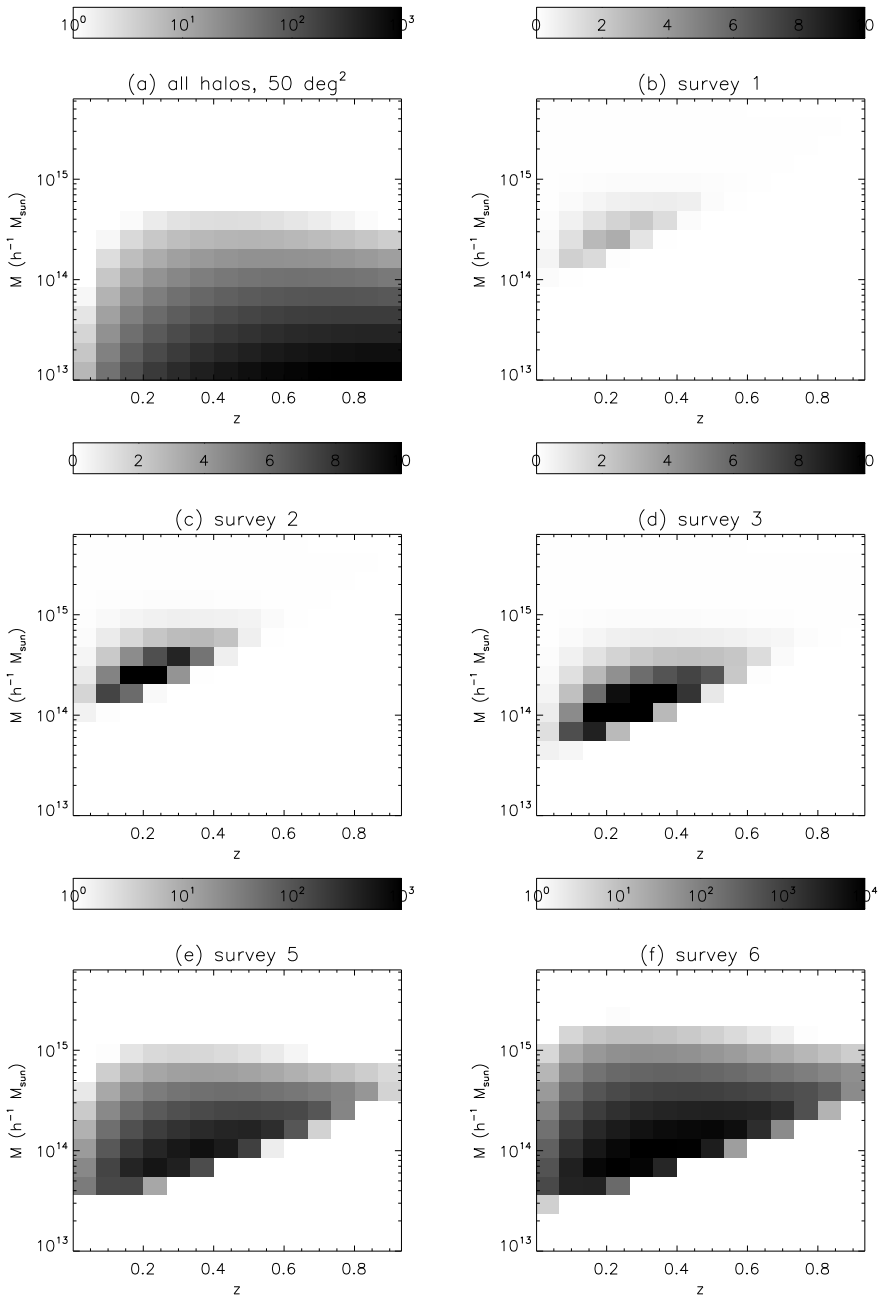

Figure 5: Absolute number of detectable halos in the mass-redshift plane for different survey configurations. (a) All clusters with mass greater than $10^{13}h^{-1}M_{\odot}$ are assumed to be detected on a 50 deg^2 survey. Other panels : all clusters with signal-to-noise ratio greater than 3 are assumed to be detected, for surveys as defined in Table 1. The difference between panels (b) and (c) comes from the different area of surveys 1 and 2, the number of halos increasing linearly with area. Panels (b) and (d) differ by the selection function associated with surveys 1 and 3 : less massive and farther clusters are detectable with survey 3, as shown by Fig. 2. The same effect is seeable when shifting to panels (e) and (f). The difference between panels (e) and (f) is the sky coverage only, and they compare the same way as panels (b) and (c).

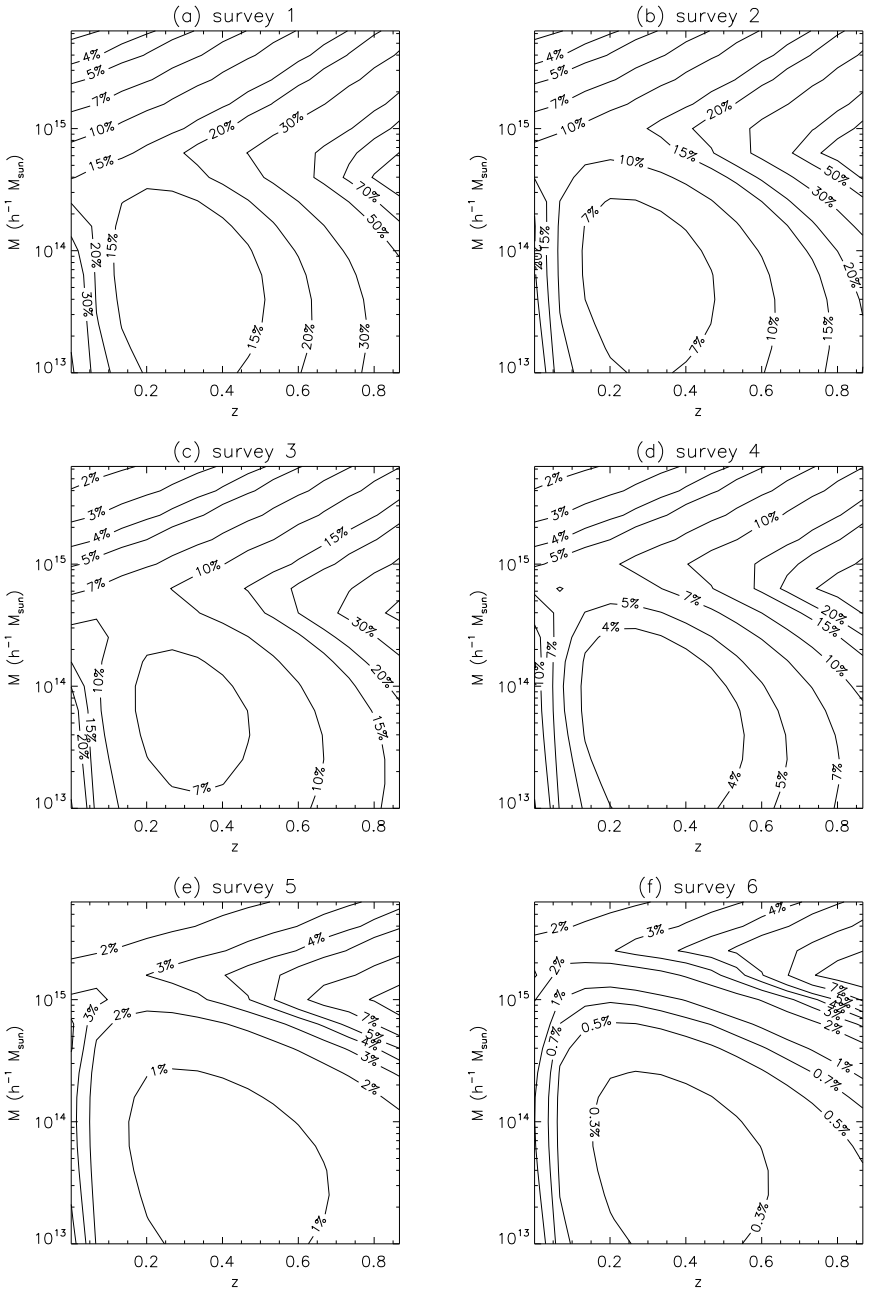

Figure 6: Relative error that can be reached on average cluster's mass measurement by stacking the weak lensing signal of identical halos (identical halos being defined as having roughly the same mass and the same redshift), in the redshift-mass plane. Stacking N clusters decreases the error on the mass measurement by a factor $\sqrt{N}$ (e.g. [4]). From top to bottom and left to right, panels correspond to surveys 1 through 6 as defined in Table 1. In this figure, we assume that all clusters with mass greater than $10^{13}h^{-1}M_{\odot}$ ($T \geqslant 1$ keV) are detected through their X-ray signal, then that their weak lensing signals are stacked in thin bins of mass and redshift (we divided the redshift-mass plane shown in the figure into 15 mass bins and 15 redshift bins). The bins size affects the measurement in that way : big bins allows us to stack more clusters, and to lower the error, but the identical halos hypothesis does not longer hold. The contour patterns reflect the combination of the abundance of clusters in the mass-redshift plane (Fig. 5(a)). The upper part of each panel corresponds to the error made on the mass measurement of a single cluster (Fig. 4), since at most one such halo can be detected in each mass-redshift bin in those regions.

References

[1] Bergé J. et al., 2008, MNRAS, in press, astro-ph/0712.3293

[2] Bergé J. et al., in prep

[3] Jenkins A. et al., 2001, MNRAS, 321, 372

[4] Sealfon C., Verde L., Jimenez R., 2006, ApJ, 649, 118

[5] Smail I. et al., 1997, ApJ, 479, 70